

CERN-PH-EP-2010-060

Submitted to: PRL

Charged-particle multiplicity density at mid-rapidity in central Pb–Pb collisions at $\sqrt{s_{NN}} = 2.76$ TeV

ALICE Collaboration

Abstract

The first measurement of the charged-particle multiplicity density at mid-rapidity in Pb–Pb collisions at a centre-of-mass energy per nucleon pair $\sqrt{s_{NN}} = 2.76$ TeV is presented. For an event sample corresponding to the most central 5% of the hadronic cross section the pseudo-rapidity density of primary charged particles at mid-rapidity is 1584 ± 4 (*stat.*) ± 76 (*sys.*), which corresponds to 8.3 ± 0.4 (*sys.*) per participating nucleon pair. This represents an increase of about a factor 1.9 relative to pp collisions at similar collision energies, and about a factor 2.2 to central Au–Au collisions at $\sqrt{s_{NN}} = 0.2$ TeV. This measurement provides the first experimental constraint for models of nucleus–nucleus collisions at LHC energies.

**Charged-particle multiplicity density at mid-rapidity
in central Pb–Pb collisions at $\sqrt{s_{NN}} = 2.76$ TeV**

(ALICE Collaboration)

K. Aamodt,¹ B. Abelev,² A. Abrahantes Quintana,³ D. Adamová,⁴ A.M. Adare,⁵ M.M. Aggarwal,⁶
G. Aglieri Rinella,⁷ A.G. Agocs,⁸ S. Aguilar Salazar,⁹ Z. Ahammed,¹⁰ A. Ahmad Masoodi,¹¹ N. Ahmad,¹¹
S.U. Ahn,^{12, a} A. Akindinov,¹³ D. Aleksandrov,¹⁴ B. Alessandro,¹⁵ R. Alfaro Molina,⁹ A. Alici,^{16, b}
A. Alkin,¹⁷ E. Almaráz Aviña,⁹ T. Alt,¹⁸ V. Altini,¹⁹ S. Altinpinar,²⁰ I. Altsybeev,²¹ C. Andrei,²²
A. Andronic,²⁰ V. Anguelov,^{23, c} C. Anson,²⁴ T. Antičić,²⁵ F. Antinori,²⁶ P. Antonioli,²⁷ L. Aphecetche,²⁸
H. Appelshäuser,²⁹ N. Arbor,³⁰ S. Arcelli,¹⁶ A. Arend,²⁹ N. Armesto,³¹ R. Arnaldi,¹⁵ T. Aronsson,⁵ I.C. Arsene,²⁰
A. Asryan,²¹ A. Augustinus,⁷ R. Averbeck,²⁰ T.C. Awes,³² J. Äystö,³³ M.D. Azmi,¹¹ M. Bach,¹⁸ A. Badalà,³⁴
Y.W. Baek,¹² S. Bagnasco,¹⁵ R. Bailhache,²⁹ R. Bala,^{35, d} R. Baldini Ferroli,³⁶ A. Baldisseri,³⁷ A. Baldit,³⁸
F. Baltasar Dos Santos Pedrosa,⁷ J. Bán,³⁹ R. Barbera,⁴⁰ F. Barile,¹⁹ G.G. Barnaföldi,⁸ L.S. Barnby,⁴¹
V. Barret,³⁸ J. Bartke,⁴² M. Basile,¹⁶ N. Bastid,³⁸ B. Bathen,⁴³ G. Batigne,²⁸ B. Batyunya,⁴⁴ C. Baumann,²⁹
I.G. Bearden,⁴⁵ H. Beck,²⁹ I. Belikov,⁴⁶ F. Bellini,¹⁶ R. Bellwied,^{47, e} E. Belmont-Moreno,⁹ S. Beole,³⁵
I. Berceanu,²² A. Bercuci,²² E. Berdermann,²⁰ Y. Berdnikov,⁴⁸ C. Bergmann,⁴³ L. Betev,⁷ A. Bhasin,⁴⁹
A.K. Bhati,⁶ L. Bianchi,³⁵ N. Bianchi,⁵⁰ C. Bianchin,²⁶ J. Bielčák,⁵¹ J. Bielčíková,⁴ A. Bilandžić,⁵² E. Biolcati,³⁵
A. Blanc,³⁸ F. Blanco,⁵³ F. Blanco,⁵⁴ D. Blau,¹⁴ C. Blume,²⁹ M. Boccioni,⁷ N. Bock,²⁴ A. Bogdanov,⁵⁵ H. Bøggild,⁴⁵
M. Bogolyubsky,⁵⁶ L. Boldizsár,⁸ M. Bombara,⁵⁷ C. Bombonati,²⁶ J. Book,²⁹ H. Borel,³⁷ A. Borissov,⁴⁷
C. Bortolin,^{26, f} S. Bose,⁵⁸ F. Bossú,³⁵ M. Botje,⁵² S. Böttger,²³ B. Boyer,⁵⁹ P. Braun-Munzinger,²⁰ L. Bravina,⁶⁰
M. Bregant,^{61, g} T. Breitner,²³ M. Broz,⁶² R. Brun,⁷ E. Bruna,⁵ G.E. Bruno,¹⁹ D. Budnikov,⁶³ H. Buesching,²⁹
K. Bugaiev,¹⁷ O. Busch,⁶⁴ Z. Buthelezi,⁶⁵ D. Caffarri,²⁶ X. Cai,⁶⁶ H. Caines,⁵ E. Calvo Villar,⁶⁷ P. Camerini,⁶¹
V. Canoa Roman,^{7, h} G. Cara Romeo,²⁷ F. Carena,⁷ W. Carena,⁷ F. Carminati,⁷ A. Casanova Díaz,⁵⁰ M. Caselle,⁷
J. Castillo Castellanos,³⁷ V. Catanesu,²² C. Cavicchioli,⁷ J. Cepila,⁵¹ P. Cerello,¹⁵ B. Chang,³³ S. Chapeland,⁷
J.L. Charvet,³⁷ S. Chattopadhyay,⁵⁸ S. Chattopadhyay,¹⁰ M. Cherney,⁶⁸ C. Cheshkov,⁶⁹ B. Cheynis,⁶⁹
E. Chiavassa,¹⁵ V. Chibante Barroso,⁷ D.D. Chinellato,⁷⁰ P. Chochula,⁷ M. Chojnacki,⁷¹ P. Christakoglou,⁷¹
C.H. Christensen,⁴⁵ P. Christiansen,⁷² T. Chujo,⁷³ C. Cicalo,⁷⁴ L. Cifarelli,¹⁶ F. Cindolo,²⁷ J. Cleymans,⁶⁵
F. Coccetti,³⁶ J.-P. Coffin,⁴⁶ S. Coli,¹⁵ G. Conesa Balbastre,^{50, i} Z. Conesa del Valle,^{28, j} P. Constantin,⁶⁴
G. Contin,⁶¹ J.G. Contreras,⁷⁵ T.M. Cormier,⁴⁷ Y. Corrales Morales,³⁵ I. Cortés Maldonado,⁷⁶ P. Cortese,⁷⁷
M.R. Cosentino,⁷⁰ F. Costa,⁷ M.E. Cotallo,⁵³ E. Crescio,⁷⁵ P. Crochet,³⁸ E. Cuautle,⁷⁸ L. Cunqueiro,⁵⁰
G. D'Erasmus,¹⁹ A. Dainese,^{79, k} H.H. Dalgaard,⁴⁵ A. Danu,⁸⁰ D. Das,⁵⁸ I. Das,⁵⁸ K. Das,⁵⁸ A. Dash,⁸¹ S. Dash,¹⁵
S. De,¹⁰ A. De Azevedo Moregula,⁵⁰ G.O.V. de Barros,⁸² A. De Caro,⁸³ G. de Cataldo,⁸⁴ J. de Cuveland,¹⁸
A. De Falco,⁸⁵ D. De Gruttola,⁸³ N. De Marco,¹⁵ S. De Pasquale,⁸³ R. De Remigis,¹⁵ R. de Rooij,⁷¹ P.R. Debski,⁸⁶
E. Del Castillo Sanchez,⁷ H. Delagrange,²⁸ Y. Delgado Mercado,⁶⁷ G. Dellacasa,^{77, l} A. Deloff,⁸⁶ V. Demanov,⁶³
E. Dénes,⁸ A. Deppman,⁸² D. Di Bari,¹⁹ C. Di Giglio,¹⁹ S. Di Liberto,⁸⁷ A. Di Mauro,⁷ P. Di Nezza,⁵⁰ T. Dietel,⁴³
R. Divià,⁷ Ø. Djuvsland,¹ A. Dobrin,^{47, m} T. Dobrowolski,⁸⁶ I. Domínguez,⁷⁸ B. Dönigus,²⁰ O. Dordic,⁶⁰ O. Driga,²⁸
A.K. Dubey,¹⁰ J. Dubuisson,⁷ L. Ducroux,⁶⁹ P. Dupieux,³⁸ A.K. Dutta Majumdar,⁵⁸ M.R. Dutta Majumdar,¹⁰
D. Elia,⁸⁴ D. Emschermann,⁴³ H. Engel,²³ H.A. Erdal,⁸⁸ B. Espagnon,⁵⁹ M. Estienne,²⁸ S. Esumi,⁷³ D. Evans,⁴¹
S. Evrard,⁷ G. Eyyubova,⁶⁰ C.W. Fabjan,^{7, n} D. Fabris,⁸⁹ J. Faivre,³⁰ D. Falchieri,¹⁶ A. Fantoni,⁵⁰ M. Fasel,²⁰
R. Fearick,⁶⁵ A. Fedunov,⁴⁴ D. Fehlker,¹ V. Fekete,⁶² D. Felea,⁸⁰ G. Feofilov,²¹ A. Fernández Téllez,⁷⁶ A. Ferretti,³⁵
R. Ferretti,^{77, o} J. Figiel,⁴² M.A.S. Figueredo,⁸² S. Filchagin,⁶³ R. Fini,⁸⁴ D. Finogeev,⁹⁰ F.M. Fionda,¹⁹
E.M. Fiore,¹⁹ M. Floris,⁷ S. Foertsch,⁶⁵ P. Foka,²⁰ S. Fokin,¹⁴ E. Fragiaco,⁹¹ M. Fragkiadakis,⁹² U. Frankendorf,²⁰
U. Fuchs,⁷ F. Furano,⁷ C. Furget,³⁰ M. Fusco Girard,⁸³ J.J. Gaardhøje,⁴⁵ S. Gadrat,³⁰ M. Gagliardi,³⁵ A. Gago,⁶⁷
M. Gallo,³⁵ D.R. Gangadharan,²⁴ P. Ganoti,^{92, p} M.S. Ganti,¹⁰ C. Garabatos,²⁰ E. Garcia-Solis,⁹³ I. Garishvili,²
R. Gemme,⁷⁷ J. Gerhard,¹⁸ M. Germain,²⁸ C. Geuna,³⁷ A. Gheata,⁷ M. Gheata,⁷ B. Ghidini,¹⁹ P. Ghosh,¹⁰
P. Gianotti,⁵⁰ M.R. Girard,⁹⁴ G. Giraudo,¹⁵ P. Giubellino,^{35, q} E. Gladysz-Dziadus,⁴² P. Glässel,⁶⁴ R. Gomez,⁹⁵
E.G. Ferreira,³¹ H. González Santos,⁷⁶ L.H. González-Trueba,⁹ P. González-Zamora,⁵³ S. Gorbunov,¹⁸ S. Gotovac,⁹⁶
V. Grabski,⁹ R. Grajcarek,⁶⁴ A. Grelli,⁷¹ A. Grigoras,⁷ C. Grigoras,⁷ V. Grigoriev,⁵⁵ A. Grigoryan,⁹⁷
S. Grigoryan,⁴⁴ B. Grinyov,¹⁷ N. Grion,⁹¹ P. Gros,⁷² J.F. Grosse-Oetringhaus,⁷ J.-Y. Grossiord,⁶⁹ R. Grosso,⁸⁹
F. Guber,⁹⁰ R. Guernane,³⁰ C. Guerra Gutierrez,⁶⁷ B. Guerzoni,¹⁶ K. Gulbrandsen,⁴⁵ T. Gunji,⁹⁸ A. Gupta,⁴⁹
R. Gupta,⁴⁹ H. Gutbrod,²⁰ Ø. Haaland,¹ C. Hadjidakis,⁵⁹ M. Haiduc,⁸⁰ H. Hamagaki,⁹⁸ G. Hamar,⁸ J.W. Harris,⁵

M. Hartig,²⁹ D. Hasch,⁵⁰ D. Hasegan,⁸⁰ D. Hatzifotiadou,²⁷ A. Hayrapetyan,^{97, o} M. Heide,⁴³ M. Heinz,⁵ H. Helstrup,⁸⁸ A. Hergehelegiu,²² C. Hernández,²⁰ G. Herrera Corral,⁷⁵ N. Herrmann,⁶⁴ K.F. Hetland,⁸⁸ B. Hicks,⁵ P.T. Hille,⁵ B. Hippolyte,⁴⁶ T. Horaguchi,⁷³ Y. Hori,⁹⁸ P. Hristov,⁷ I. Hřivnáčová,⁵⁹ M. Huang,¹ S. Huber,²⁰ T.J. Humanic,²⁴ D.S. Hwang,⁹⁹ R. Ichou,²⁸ R. Ilkaev,⁶³ I. Ilkiv,⁸⁶ M. Inaba,⁷³ E. Incani,⁸⁵ G.M. Innocenti,³⁵ P.G. Innocenti,⁷ M. Ippolitov,¹⁴ M. Irfan,¹¹ C. Ivan,²⁰ A. Ivanov,²¹ M. Ivanov,²⁰ V. Ivanov,⁴⁸ A. Jacholkowski,⁷ P. M. Jacobs,¹⁰⁰ L. Jancurová,⁴⁴ S. Jangal,⁴⁶ R. Janik,⁶² S. Jena,¹⁰¹ L. Jirden,⁷ G.T. Jones,⁴¹ P.G. Jones,⁴¹ P. Jovanović,⁴¹ H. Jung,¹² W. Jung,¹² A. Jusko,⁴¹ S. Kalcher,¹⁸ P. Kaliňák,³⁹ M. Kalisky,⁴³ T. Kalliokoski,³³ A. Kalweit,¹⁰² R. Kamermans,^{71, l} K. Kanaki,¹ E. Kang,¹² J.H. Kang,¹⁰³ V. Kaplin,⁵⁵ O. Karavichev,⁹⁰ T. Karavicheva,⁹⁰ E. Karpechev,⁹⁰ A. Kazantsev,¹⁴ U. Keschull,²³ R. Keidel,¹⁰⁴ M.M. Khan,¹¹ S.A. Khan,¹⁰ A. Khanzadeev,⁴⁸ Y. Kharlov,⁵⁶ B. Kileng,⁸⁸ D.J. Kim,³³ D.S. Kim,¹² D.W. Kim,¹² H.N. Kim,¹² J.H. Kim,⁹⁹ J.S. Kim,¹² M. Kim,¹² M. Kim,¹⁰³ S. Kim,⁹⁹ S.H. Kim,¹² S. Kirsch,^{7, r} I. Kisel,^{23, s} S. Kiselev,¹³ A. Kisiel,⁷ J.L. Klay,¹⁰⁵ J. Klein,⁶⁴ C. Klein-Bösing,⁴³ M. Kliemant,²⁹ A. Klovning,¹ A. Kluge,⁷ M.L. Knichel,²⁰ K. Koch,⁶⁴ M.K. Köhler,²⁰ R. Kolevatov,⁶⁰ A. Kolojvari,²¹ V. Kondratiev,²¹ N. Kondratyeva,⁵⁵ A. Konevskih,⁹⁰ E. Kornaš,⁴² C. Kottachchi Kankanamge Don,⁴⁷ R. Kour,⁴¹ M. Kowalski,⁴² S. Kox,³⁰ G. Koyithatta Meethalevedu,¹⁰¹ K. Kozlov,¹⁴ J. Kral,³³ I. Králik,³⁹ F. Kramer,²⁹ I. Kraus,^{102, t} T. Krawutschke,^{64, u} M. Kretz,¹⁸ M. Krivda,^{41, v} F. Krizek,³³ D. Krumbhorn,⁶⁴ M. Krus,⁵¹ E. Kryshen,⁴⁸ M. Krzewicki,⁵² Y. Kucheriaev,¹⁴ C. Kuhn,⁴⁶ P.G. Kuijer,⁵² P. Kurashvili,⁸⁶ A. Kurepin,⁹⁰ A.B. Kurepin,⁹⁰ A. Kuryakin,⁶³ S. Kushpil,⁴ V. Kushpil,⁴ M.J. Kweon,⁶⁴ Y. Kwon,¹⁰³ P. La Rocca,⁴⁰ P. Ladrón de Guevara,^{53, w} V. Lafage,⁵⁹ C. Lara,²³ A. Lardeux,²⁸ D.T. Larsen,¹ C. Lazzeroni,⁴¹ Y. Le Bornec,⁵⁹ R. Lea,⁶¹ K.S. Lee,¹² S.C. Lee,¹² F. Lefèvre,²⁸ J. Lehnert,²⁹ L. Leistam,⁷ M. Lenhardt,²⁸ V. Lenti,⁸⁴ I. León Monzón,⁹⁵ H. León Vargas,²⁹ P. Lévai,⁸ X. Li,¹⁰⁶ J. Lien,¹ R. Lietava,⁴¹ S. Lindal,⁶⁰ V. Lindenstruth,^{23, s} C. Lippmann,^{7, t} M.A. Lisa,²⁴ L. Liu,¹ P.I. Loenne,¹ V.R. Loggins,⁴⁷ V. Loginov,⁵⁵ S. Lohn,⁷ C. Loizides,¹⁰⁰ K.K. Loo,³³ X. Lopez,³⁸ M. López Noriega,⁵⁹ E. López Torres,³ G. Løvholden,⁶⁰ X.-G. Lu,⁶⁴ P. Luettig,²⁹ M. Lunardon,²⁶ G. Luparello,³⁵ L. Luquin,²⁸ C. Luzzi,⁷ K. Ma,⁶⁶ R. Ma,⁵ D.M. Madagadahettige-Don,⁵⁴ A. Maevskaya,⁹⁰ M. Mager,⁷ D.P. Mahapatra,⁸¹ A. Maire,⁴⁶ D. Mal'Kevich,¹³ M. Malaev,⁴⁸ I. Maldonado Cervantes,⁷⁸ L. Malinina,^{44, x} P. Malzacher,²⁰ A. Mamonov,⁶³ L. Manceau,³⁸ L. Mangotra,⁴⁹ V. Manko,¹⁴ F. Manso,³⁸ V. Manzari,⁸⁴ Y. Mao,^{66, y} J. Mareš,¹⁰⁷ G.V. Margagliotti,⁶¹ A. Margotti,²⁷ A. Marín,²⁰ C. Markert,¹⁰⁸ I. Martashvili,¹⁰⁹ P. Martinengo,⁷ M.I. Martínez,⁷⁶ A. Martínez Davalos,⁹ G. Martínez García,²⁸ Y. Martynov,¹⁷ S. Masciocchi,²⁰ M. Maserà,³⁵ A. Masoni,⁷⁴ L. Massacrier,⁶⁹ M. Mastroarco,⁸⁴ A. Mastroserio,⁷ Z.L. Matthews,⁴¹ A. Matyja,²⁸ D. Mayani,⁷⁸ C. Mayer,⁴² G. Mazza,¹⁵ M.A. Mazzoni,⁸⁷ F. Meddi,¹¹⁰ A. Menchaca-Rocha,⁹ P. Mendez Lorenzo,⁷ I. Menis,⁹² J. Mercado Pérez,⁶⁴ M. Meres,⁶² P. Mereu,¹⁵ Y. Miake,⁷³ J. Midori,¹¹¹ L. Milano,³⁵ J. Milosevic,^{60, z} A. Mischke,⁷¹ D. Miśkowiec,^{20, q} C. Mitu,⁸⁰ J. Mlynarz,⁴⁷ A.K. Mohanty,⁷ B. Mohanty,¹⁰ L. Molnar,⁷ L. Montaña Zetina,⁷⁵ M. Monteno,¹⁵ E. Montes,⁵³ M. Morando,²⁶ D.A. Moreira De Godoy,⁸² S. Moretto,²⁶ A. Morsch,⁷ V. Muccifora,⁵⁰ E. Mudnic,⁹⁶ S. Muhuri,¹⁰ H. Müller,⁷ M.G. Munhoz,⁸² J. Munoz,⁷⁶ L. Musa,⁷ A. Musso,¹⁵ B.K. Nandi,¹⁰¹ R. Nania,²⁷ E. Nappi,⁸⁴ C. Natrass,¹⁰⁹ F. Navach,¹⁹ S. Navin,⁴¹ T.K. Nayak,¹⁰ S. Nazarenko,⁶³ G. Nazarov,⁶³ A. Nedosekin,¹³ F. Nendaz,⁶⁹ J. Newby,² M. Nicassio,¹⁹ B.S. Nielsen,⁴⁵ T. Niida,⁷³ S. Nikolaev,¹⁴ V. Nikolic,²⁵ S. Nikulin,¹⁴ V. Nikulin,⁴⁸ B.S. Nilsen,⁶⁸ M.S. Nilsson,⁶⁰ F. Noferini,²⁷ G. Nooren,⁷¹ N. Novitzky,³³ A. Nyanin,¹⁴ A. Nyatha,¹⁰¹ C. Nygaard,⁴⁵ J. Nystrand,¹ H. Obayashi,¹¹¹ A. Ochirov,²¹ H. Oeschler,¹⁰² S.K. Oh,¹² J. Oleniacz,⁹⁴ C. Oppedisano,¹⁵ A. Ortiz Velasquez,⁷⁸ G. Ortona,³⁵ A. Oskarsson,⁷² P. Ostrowski,⁹⁴ I. Otterlund,⁷² J. Otwinowski,²⁰ K. Oyama,⁶⁴ K. Ozawa,⁹⁸ Y. Pachmayer,⁶⁴ M. Pachr,⁵¹ F. Padilla,³⁵ P. Pagano,⁸³ S.P. Jayarathna,^{54, aa} G. Paic,⁷⁸ F. Painke,¹⁸ C. Pajares,³¹ S. Pal,³⁷ S.K. Pal,¹⁰ A. Palaha,⁴¹ A. Palmeri,³⁴ G.S. Pappalardo,³⁴ W.J. Park,²⁰ D.I. Patalakha,⁵⁶ V. Paticchio,⁸⁴ A. Pavlinov,⁴⁷ T. Pawlak,⁹⁴ T. Peitzmann,⁷¹ D. Peresunko,¹⁴ C.E. Pérez Lara,⁵² D. Perini,⁷ D. Perrino,¹⁹ W. Peryt,⁹⁴ A. Pesci,²⁷ V. Peskov,⁷ Y. Pestov,¹¹² A.J. Peters,⁷ V. Petráček,⁵¹ M. Petran,⁵¹ M. Petris,²² P. Petrov,⁴¹ M. Petrovici,²² C. Petta,⁴⁰ S. Piano,⁹¹ A. Piccotti,¹⁵ M. Pikna,⁶² P. Pillot,²⁸ O. Pinazza,⁷ L. Pinsky,⁵⁴ N. Pitz,²⁹ F. Piuz,⁷ D.B. Piyarathna,^{47, bb} R. Platt,⁴¹ M. Płoskoń,¹⁰⁰ J. Pluta,⁹⁴ T. Pocheptsov,^{44, cc} S. Pochybova,⁸ P.L.M. Podesta-Lerma,⁹⁵ M.G. Poghosyan,³⁵ K. Polák,¹⁰⁷ B. Polichtchouk,⁵⁶ A. Pop,²² S. Porteboeuf,³⁸ V. Pospíšil,⁵¹ B. Potukuchi,⁴⁹ S.K. Prasad,^{47, dd} R. Preghenella,³⁶ F. Prino,¹⁵ C.A. Pruneau,⁴⁷ I. Pshenichnov,⁹⁰ G. Puddu,⁸⁵ A. Pulvirenti,⁴⁰ V. Punin,⁶³ M. Putiš,⁵⁷ J. Putschke,⁵ E. Quercigh,⁷ H. Qvigstad,⁶⁰ A. Rachevski,⁹¹ A. Rademakers,⁷ O. Rademakers,⁷ S. Radomski,⁶⁴ T.S. Rähjä,³³ J. Rak,³³ A. Rakotozafindrabe,³⁷ L. Ramello,⁷⁷ A. Ramírez Reyes,⁷⁵ M. Rammler,⁴³ R. Raniwala,¹¹³ S. Raniwala,¹¹³ S.S. Räsänen,³³ K.F. Read,¹⁰⁹ J. Real,³⁰ K. Redlich,⁸⁶ R. Renfordt,²⁹ A.R. Reolon,⁵⁰ A. Reshetin,⁹⁰ F. Rettig,¹⁸ J.-P. Revol,⁷ K. Reygers,⁶⁴ H. Ricaud,¹⁰²

L. Riccati,¹⁵ R.A. Ricci,⁷⁹ M. Richter,^{1, ee} P. Riedler,⁷ W. Riegler,⁷ F. Riggi,⁴⁰ M. Rodríguez Cahuantzi,⁷⁶
D. Rohr,¹⁸ D. Röhrich,¹ R. Romita,²⁰ F. Ronchetti,⁵⁰ P. Rosinský,⁷ P. Rosnet,³⁸ S. Rossegger,⁷ A. Rossi,²⁶
F. Roukoutakis,⁹² S. Rousseau,⁵⁹ C. Roy,^{28, j} P. Roy,⁵⁸ A.J. Rubio Montero,⁵³ R. Rui,⁶¹ A. Rivetti,¹⁵ I. Rusanov,⁷
E. Ryabinkin,¹⁴ A. Rybicki,⁴² S. Sadovsky,⁵⁶ K. Šafařík,⁷ R. Sahoo,²⁶ P.K. Sahu,⁸¹ J. Saini,¹⁰ P. Saiz,⁷ S. Sakai,¹⁰⁰
D. Sakata,⁷³ C.A. Salgado,³¹ T. Samanta,¹⁰ S. Sambyal,⁴⁹ V. Samsonov,⁴⁸ X. Sanchez Castro,⁷⁸ L. Šándor,³⁹
A. Sandoval,⁹ M. Sano,⁷³ S. Sano,⁹⁸ R. Santo,⁴³ R. Santoro,⁸⁴ J. Sarkamo,³³ P. Saturnini,³⁸ E. Scapparone,²⁷
F. Scarlassara,²⁶ R.P. Scharenberg,¹¹⁴ C. Schiaua,²² R. Schicker,⁶⁴ C. Schmidt,²⁰ H.R. Schmidt,²⁰ S. Schreiner,⁷
S. Schuchmann,²⁹ J. Schukraft,⁷ Y. Schutz,²⁸ K. Schwarz,²⁰ K. Schweda,⁶⁴ G. Scioli,¹⁶ E. Scomparin,¹⁵ P.A. Scott,⁴¹
R. Scott,¹⁰⁹ G. Segato,²⁶ I. Selyuzhenkov,²⁰ S. Senyukov,⁷⁷ J. Seo,¹² S. Serici,⁸⁵ E. Serradilla,⁵³ A. Sevcenco,⁸⁰
I. Sgura,⁸⁴ G. Shabratova,⁴⁴ R. Shahoyan,⁷ N. Sharma,⁶ S. Sharma,⁴⁹ K. Shigaki,¹¹¹ M. Shimomura,⁷³ K. Shtejer,³
Y. Sibirak,¹⁴ M. Siciliano,³⁵ E. Sicking,⁷ T. Siemiarczuk,⁸⁶ A. Silenzi,¹⁶ D. Silvermyr,³² G. Simonetti,^{7, ff}
R. Singaraju,¹⁰ R. Singh,⁴⁹ V. Singhal,¹⁰ B.C. Sinha,¹⁰ T. Sinha,⁵⁸ B. Sitar,⁶² M. Sitta,⁷⁷ T.B. Skaali,⁶⁰
K. Skjerdal,¹ R. Smakal,⁵¹ N. Smirnov,⁵ R. Snellings,^{52, gg} C. Sogaard,⁴⁵ A. Soloviev,⁵⁶ R. Soltz,² H. Son,⁹⁹
J. Song,¹¹⁵ M. Song,¹⁰³ C. Soos,⁷ F. Soramel,²⁶ M. Spyropoulou-Stassinaki,⁹² B.K. Srivastava,¹¹⁴ J. Stachel,⁶⁴
I. Stan,⁸⁰ G. Stefanek,⁸⁶ G. Stefanini,⁷ T. Steinbeck,^{23, s} M. Steinpreis,²⁴ E. Stenlund,⁷² G. Steyn,⁶⁵ D. Stocco,²⁸
R. Stock,²⁹ C.H. Stokkevag,¹ M. Stolpovskiy,⁵⁶ P. Strmen,⁶² A.A.P. Suaide,⁸² M.A. Subieta Vásquez,³⁵
T. Sugitate,¹¹¹ C. Suire,⁵⁹ M. Sukhorukov,⁶³ M. Šumbera,⁴ T. Susa,²⁵ D. Swoboda,⁷ T.J.M. Symons,¹⁰⁰
A. Szanto de Toledo,⁸² I. Szarka,⁶² A. Szostak,¹ C. Tagridis,⁹² J. Takahashi,⁷⁰ J.D. Tapia Takaki,⁵⁹ A. Tauro,⁷
M. Tavlet,⁷ G. Tejada Muñoz,⁷⁶ A. Telesca,⁷ C. Terrevoli,¹⁹ J. Thäder,²⁰ D. Thomas,⁷¹ J.H. Thomas,²⁰
R. Tieulent,⁶⁹ A.R. Timmins,^{47, e} D. Tlusty,⁵¹ A. Toia,⁷ H. Torii,¹¹¹ L. Toscano,⁷ F. Tosello,¹⁵ T. Traczyk,⁹⁴
D. Truesdale,²⁴ W.H. Trzaska,³³ T. Tsuji,⁹⁸ A. Tumkin,⁶³ R. Turrisi,⁸⁹ A.J. Turvey,⁶⁸ T.S. Tveter,⁶⁰
J. Ulery,²⁹ K. Ullaland,¹ A. Uras,⁸⁵ J. Urbán,⁵⁷ G.M. Urciuoli,⁸⁷ G.L. Usai,⁸⁵ A. Vacchi,⁹¹ M. Vajzer,⁵¹
M. Vala,^{44, v} L. Valencia Palomo,^{9, hh} S. Vallero,⁶⁴ N. van der Kolk,⁵² M. van Leeuwen,⁷¹ P. Vande Vyvre,⁷
L. Vannucci,⁷⁹ A. Vargas,⁷⁶ R. Varma,¹⁰¹ M. Vasileiou,⁹² A. Vasiliev,¹⁴ V. Vechernin,²¹ M. Veldhoen,⁷¹
M. Venaruzzo,⁶¹ E. Vercellin,³⁵ S. Vergara,⁷⁶ D.C. Vernekohl,⁴³ R. Vernet,¹¹⁶ M. Verweij,⁷¹ L. Vickovic,⁹⁶
G. Viesti,²⁶ O. Vikhlyantsev,⁶³ Z. Vilakazi,⁶⁵ O. Villalobos Baillie,⁴¹ A. Vinogradov,¹⁴ L. Vinogradov,²¹
Y. Vinogradov,⁶³ T. Virgili,⁸³ Y.P. Viyogi,¹⁰ A. Vodopyanov,⁴⁴ K. Voloshin,¹³ S. Voloshin,⁴⁷ G. Volpe,¹⁹
B. von Haller,⁷ D. Vranic,²⁰ G. Øvrebek,¹ J. Vrláková,⁵⁷ B. Vulpescu,³⁸ A. Vyushin,⁶³ B. Wagner,¹ V. Wagner,⁵¹
R. Wan,^{46, ii} D. Wang,⁶⁶ Y. Wang,⁶⁴ Y. Wang,⁶⁶ K. Watanabe,⁷³ J.P. Wessels,⁴³ U. Westerhoff,⁴³
J. Wiechula,⁶⁴ J. Wikne,⁶⁰ M. Wilde,⁴³ A. Wilk,⁴³ G. Wilk,⁸⁶ M.C.S. Williams,²⁷ B. Windelband,⁶⁴
L. Xaplanteris Karampatsos,¹⁰⁸ H. Yang,³⁷ S. Yang,¹ S. Yasnopolskiy,¹⁴ J. Yi,¹¹⁵ Z. Yin,⁶⁶ H. Yokoyama,⁷³
I.-K. Yoo,¹¹⁵ W. Yu,²⁹ X. Yuan,⁶⁶ I. Yushmanov,¹⁴ E. Zabrodin,⁶⁰ C. Zach,⁵¹ C. Zampolli,⁷ S. Zaporozhets,⁴⁴
A. Zarochentsev,²¹ P. Závada,¹⁰⁷ N. Zaviyalov,⁶³ H. Zbroszczyk,⁹⁴ P. Zelniczek,²³ A. Zenin,⁵⁶ I. Zgura,⁸⁰
M. Zhalov,⁴⁸ X. Zhang,^{66, a} D. Zhou,⁶⁶ A. Zichichi,^{16, jj} G. Zinovjev,¹⁷ Y. Zoccarato,⁶⁹ and M. Zynovyev¹⁷

¹Department of Physics and Technology, University of Bergen, Bergen, Norway

²Lawrence Livermore National Laboratory, Livermore, California, United States

³Centro de Aplicaciones Tecnológicas y Desarrollo Nuclear (CEADEN), Havana, Cuba

⁴Nuclear Physics Institute, Academy of Sciences of the Czech Republic, Řež u Prahy, Czech Republic

⁵Yale University, New Haven, Connecticut, United States

⁶Physics Department, Panjab University, Chandigarh, India

⁷European Organization for Nuclear Research (CERN), Geneva, Switzerland

⁸KFKI Research Institute for Particle and Nuclear Physics,
Hungarian Academy of Sciences, Budapest, Hungary

⁹Instituto de Física, Universidad Nacional Autónoma de México, Mexico City, Mexico

¹⁰Variable Energy Cyclotron Centre, Kolkata, India

¹¹Department of Physics Aligarh Muslim University, Aligarh, India

¹²Gangneung-Wonju National University, Gangneung, South Korea

¹³Institute for Theoretical and Experimental Physics, Moscow, Russia

¹⁴Russian Research Centre Kurchatov Institute, Moscow, Russia

¹⁵Sezione INFN, Turin, Italy

¹⁶Dipartimento di Fisica dell'Università and Sezione INFN, Bologna, Italy

¹⁷Bogolyubov Institute for Theoretical Physics, Kiev, Ukraine

¹⁸Frankfurt Institute for Advanced Studies, Johann Wolfgang Goethe-Universität Frankfurt, Frankfurt, Germany

¹⁹Dipartimento Interateneo di Fisica 'M. Merlin' and Sezione INFN, Bari, Italy

- ²⁰ *Research Division and ExtreMe Matter Institute EMMI,
GSI Helmholtzzentrum für Schwerionenforschung, Darmstadt, Germany*
- ²¹ *V. Fock Institute for Physics, St. Petersburg State University, St. Petersburg, Russia*
- ²² *National Institute for Physics and Nuclear Engineering, Bucharest, Romania*
- ²³ *Kirchhoff-Institut für Physik, Ruprecht-Karls-Universität Heidelberg, Heidelberg, Germany*
- ²⁴ *Department of Physics, Ohio State University, Columbus, Ohio, United States*
- ²⁵ *Rudjer Bošković Institute, Zagreb, Croatia*
- ²⁶ *Dipartimento di Fisica dell'Università and Sezione INFN, Padova, Italy*
- ²⁷ *Sezione INFN, Bologna, Italy*
- ²⁸ *SUBATECH, Ecole des Mines de Nantes, Université de Nantes, CNRS-IN2P3, Nantes, France*
- ²⁹ *Institut für Kernphysik, Johann Wolfgang Goethe-Universität Frankfurt, Frankfurt, Germany*
- ³⁰ *Laboratoire de Physique Subatomique et de Cosmologie (LPSC), Université Joseph Fourier,
CNRS-IN2P3, Institut Polytechnique de Grenoble, Grenoble, France*
- ³¹ *Departamento de Física de Partículas and IGFAE,
Universidad de Santiago de Compostela, Santiago de Compostela, Spain*
- ³² *Oak Ridge National Laboratory, Oak Ridge, Tennessee, United States*
- ³³ *Helsinki Institute of Physics (HIP) and University of Jyväskylä, Jyväskylä, Finland*
- ³⁴ *Sezione INFN, Catania, Italy*
- ³⁵ *Dipartimento di Fisica Sperimentale dell'Università and Sezione INFN, Turin, Italy*
- ³⁶ *Centro Fermi – Centro Studi e Ricerche e Museo Storico della Fisica “Enrico Fermi”, Rome, Italy*
- ³⁷ *Commissariat à l’Energie Atomique, IRFU, Saclay, France*
- ³⁸ *Laboratoire de Physique Corpusculaire (LPC), Clermont Université,
Université Blaise Pascal, CNRS-IN2P3, Clermont-Ferrand, France*
- ³⁹ *Institute of Experimental Physics, Slovak Academy of Sciences, Košice, Slovakia*
- ⁴⁰ *Dipartimento di Fisica e Astronomia dell'Università and Sezione INFN, Catania, Italy*
- ⁴¹ *School of Physics and Astronomy, University of Birmingham, Birmingham, United Kingdom*
- ⁴² *The Henryk Niewodniczanski Institute of Nuclear Physics, Polish Academy of Sciences, Cracow, Poland*
- ⁴³ *Institut für Kernphysik, Westfälische Wilhelms-Universität Münster, Münster, Germany*
- ⁴⁴ *Joint Institute for Nuclear Research (JINR), Dubna, Russia*
- ⁴⁵ *Niels Bohr Institute, University of Copenhagen, Copenhagen, Denmark*
- ⁴⁶ *Institut Pluridisciplinaire Hubert Curien (IPHC),
Université de Strasbourg, CNRS-IN2P3, Strasbourg, France*
- ⁴⁷ *Wayne State University, Detroit, Michigan, United States*
- ⁴⁸ *Petersburg Nuclear Physics Institute, Gatchina, Russia*
- ⁴⁹ *Physics Department, University of Jammu, Jammu, India*
- ⁵⁰ *Laboratori Nazionali di Frascati, INFN, Frascati, Italy*
- ⁵¹ *Faculty of Nuclear Sciences and Physical Engineering,
Czech Technical University in Prague, Prague, Czech Republic*
- ⁵² *Nikhef, National Institute for Subatomic Physics, Amsterdam, Netherlands*
- ⁵³ *Centro de Investigaciones Energéticas Medioambientales y Tecnológicas (CIEMAT), Madrid, Spain*
- ⁵⁴ *University of Houston, Houston, Texas, United States*
- ⁵⁵ *Moscow Engineering Physics Institute, Moscow, Russia*
- ⁵⁶ *Institute for High Energy Physics, Protvino, Russia*
- ⁵⁷ *Faculty of Science, P.J. Šafárik University, Košice, Slovakia*
- ⁵⁸ *Saha Institute of Nuclear Physics, Kolkata, India*
- ⁵⁹ *Institut de Physique Nucléaire d’Orsay (IPNO),
Université Paris-Sud, CNRS-IN2P3, Orsay, France*
- ⁶⁰ *Department of Physics, University of Oslo, Oslo, Norway*
- ⁶¹ *Dipartimento di Fisica dell'Università and Sezione INFN, Trieste, Italy*
- ⁶² *Faculty of Mathematics, Physics and Informatics, Comenius University, Bratislava, Slovakia*
- ⁶³ *Russian Federal Nuclear Center (VNIIEF), Sarov, Russia*
- ⁶⁴ *Physikalisches Institut, Ruprecht-Karls-Universität Heidelberg, Heidelberg, Germany*
- ⁶⁵ *Physics Department, University of Cape Town,
iThemba Laboratories, Cape Town, South Africa*
- ⁶⁶ *Hua-Zhong Normal University, Wuhan, China*
- ⁶⁷ *Sección Física, Departamento de Ciencias, Pontificia Universidad Católica del Perú, Lima, Peru*
- ⁶⁸ *Physics Department, Creighton University, Omaha, Nebraska, United States*
- ⁶⁹ *Université de Lyon, Université Lyon 1, CNRS/IN2P3, IPN-Lyon, Villeurbanne, France*
- ⁷⁰ *Universidade Estadual de Campinas (UNICAMP), Campinas, Brazil*
- ⁷¹ *Nikhef, National Institute for Subatomic Physics and Institute
for Subatomic Physics of Utrecht University, Utrecht, Netherlands*
- ⁷² *Division of Experimental High Energy Physics, University of Lund, Lund, Sweden*
- ⁷³ *University of Tsukuba, Tsukuba, Japan*
- ⁷⁴ *Sezione INFN, Cagliari, Italy*

- ⁷⁵ *Centro de Investigación y de Estudios Avanzados (CINVESTAV), Mexico City and Mérida, Mexico*
⁷⁶ *Benemérita Universidad Autónoma de Puebla, Puebla, Mexico*
⁷⁷ *Dipartimento di Scienze e Tecnologie Avanzate dell'Università del Piemonte Orientale and Gruppo Collegato INFN, Alessandria, Italy*
⁷⁸ *Instituto de Ciencias Nucleares, Universidad Nacional Autónoma de México, Mexico City, Mexico*
⁷⁹ *Laboratori Nazionali di Legnaro, INFN, Legnaro, Italy*
⁸⁰ *Institute of Space Sciences (ISS), Bucharest, Romania*
⁸¹ *Institute of Physics, Bhubaneswar, India*
⁸² *Universidade de São Paulo (USP), São Paulo, Brazil*
⁸³ *Dipartimento di Fisica 'E.R. Caianiello' dell'Università and Gruppo Collegato INFN, Salerno, Italy*
⁸⁴ *Sezione INFN, Bari, Italy*
⁸⁵ *Dipartimento di Fisica dell'Università and Sezione INFN, Cagliari, Italy*
⁸⁶ *Soltan Institute for Nuclear Studies, Warsaw, Poland*
⁸⁷ *Sezione INFN, Rome, Italy*
⁸⁸ *Faculty of Engineering, Bergen University College, Bergen, Norway*
⁸⁹ *Sezione INFN, Padova, Italy*
⁹⁰ *Institute for Nuclear Research, Academy of Sciences, Moscow, Russia*
⁹¹ *Sezione INFN, Trieste, Italy*
⁹² *Physics Department, University of Athens, Athens, Greece*
⁹³ *Chicago State University, Chicago, United States*
⁹⁴ *Warsaw University of Technology, Warsaw, Poland*
⁹⁵ *Universidad Autónoma de Sinaloa, Culiacán, Mexico*
⁹⁶ *Technical University of Split FESB, Split, Croatia*
⁹⁷ *Yerevan Physics Institute, Yerevan, Armenia*
⁹⁸ *University of Tokyo, Tokyo, Japan*
⁹⁹ *Department of Physics, Sejong University, Seoul, South Korea*
¹⁰⁰ *Lawrence Berkeley National Laboratory, Berkeley, California, United States*
¹⁰¹ *Indian Institute of Technology, Mumbai, India*
¹⁰² *Institut für Kernphysik, Technische Universität Darmstadt, Darmstadt, Germany*
¹⁰³ *Yonsei University, Seoul, South Korea*
¹⁰⁴ *Zentrum für Technologietransfer und Telekommunikation (ZTT), Fachhochschule Worms, Worms, Germany*
¹⁰⁵ *California Polytechnic State University, San Luis Obispo, California, United States*
¹⁰⁶ *China Institute of Atomic Energy, Beijing, China*
¹⁰⁷ *Institute of Physics, Academy of Sciences of the Czech Republic, Prague, Czech Republic*
¹⁰⁸ *The University of Texas at Austin, Physics Department, Austin, TX, United States*
¹⁰⁹ *University of Tennessee, Knoxville, Tennessee, United States*
¹¹⁰ *Dipartimento di Fisica dell'Università 'La Sapienza' and Sezione INFN, Rome, Italy*
¹¹¹ *Hiroshima University, Hiroshima, Japan*
¹¹² *Budker Institute for Nuclear Physics, Novosibirsk, Russia*
¹¹³ *Physics Department, University of Rajasthan, Jaipur, India*
¹¹⁴ *Purdue University, West Lafayette, Indiana, United States*
¹¹⁵ *Pusan National University, Pusan, South Korea*
¹¹⁶ *Centre de Calcul de l'IN2P3, Villeurbanne, France*
- (Dated: October 2, 2017)

The first measurement of the charged-particle multiplicity density at mid-rapidity in Pb–Pb collisions at a centre-of-mass energy per nucleon pair $\sqrt{s_{NN}} = 2.76$ TeV is presented. For an event sample corresponding to the most central 5% of the hadronic cross section the pseudo-rapidity density of primary charged particles at mid-rapidity is 1584 ± 4 (*stat.*) ± 76 (*sys.*), which corresponds to 8.3 ± 0.4 (*sys.*) per participating nucleon pair. This represents an increase of about a factor 1.9 relative to pp collisions at similar collision energies, and about a factor 2.2 to central Au–Au collisions at $\sqrt{s_{NN}} = 0.2$ TeV. This measurement provides the first experimental constraint for models of nucleus–nucleus collisions at LHC energies.

^a Also at Laboratoire de Physique Corpusculaire (LPC), Clermont Université, Université Blaise Pascal, CNRS–IN2P3, Clermont-Ferrand, France;

^b Now at Centro Fermi – Centro Studi e Ricerche e Museo Storico della Fisica “Enrico Fermi”, Rome, Italy;

^c Now at Physikalisches Institut, Ruprecht-Karls-Universität Hei-

delberg, Heidelberg, Germany; Now at Frankfurt Institute for Advanced Studies, Johann Wolfgang Goethe-Universität Frankfurt, Frankfurt, Germany;

^d Now at Sezione INFN, Turin, Italy;

^e Now at University of Houston, Houston, Texas, United States;

^f Also at Dipartimento di Fisica dell'Università, Udine, Italy ;

The theory of strong interactions, Quantum Chromodynamics (QCD), predicts a phase transition at high temperature between hadronic matter, where quarks and gluons are confined inside hadrons, and a deconfined state of matter, the Quark–Gluon Plasma (QGP). A new frontier in the study of QCD matter opened with the first collisions of ^{208}Pb ions in November 2010, at the Large Hadron Collider (LHC) at CERN. These collisions are expected to generate matter at unprecedented temperatures and energy densities in the laboratory.

The first step in characterizing the system produced in these collisions is the measurement of the charged-particle pseudo-rapidity density, which constrains the dominant particle production mechanisms and is essential to estimate the initial energy density. The dependence of the charged-particle multiplicity density on energy and system size reflects the interplay between hard parton–parton scattering processes and soft processes. Predictions of models that successfully describe particle production at RHIC vary by a factor of two at the LHC [1, 2].

This Letter reports the measurement of the charged-particle pseudo-rapidity density produced in Pb–Pb collisions at the LHC, utilizing data taken with the ALICE detector [3] at a centre-of-mass energy per nucleon pair $\sqrt{s_{\text{NN}}} = 2.76$ TeV. The primary charged-particle density, $dN_{\text{ch}}/d\eta$, in central (small impact parameter) Pb–Pb collisions is measured in the pseudo-rapidity interval $|\eta| \equiv |-\ln \tan(\theta/2)| < 0.5$, where θ is the polar angle between the charged-particle direction and the beam axis (z). We define primary particles as prompt particles produced in the collision, including decay products, except those from weak decays of strange particles.

The present measurement extends the study of particle densities in nucleus–nucleus collisions into the TeV regime. We make comparisons to model predictions [4–16], and to previous measurements in nucleus–nucleus collisions at lower energies at the SPS and RHIC [17–25], as well as to pp and p \bar{p} collisions over a wide energy range [26–32]. Our measurement provides new insight into particle production mechanisms in high energy nuclear collisions and enables more precise model predictions for a wide array of other observables in nuclear collisions at the LHC.

A detailed description of the ALICE experiment is given in Ref. [3]. Here, we briefly describe the detector components used in this analysis. The Silicon Pixel Detector (SPD) is the innermost part of the Inner Tracking System (ITS). It consists of two cylindrical layers of hybrid silicon pixel assemblies positioned at radial distances of 3.9 and 7.6 cm from the beam line, with a total of 9.8×10^6 pixels of size $50 \times 425 \mu\text{m}^2$, read out by 1200 electronic chips. The SPD coverage for particles originating from the center of the detector is $|\eta| < 2.0$ and $|\eta| < 1.4$ for the inner and outer layers, respectively. Each chip provides a fast signal if at least one of its pixels is hit. The signals from the 1200 chips are combined in a programmable logic unit which supplies a trigger signal. The fraction of SPD channels active during data taking was 70% for the inner and 78% for the outer layer. The VZERO detector consists of two arrays of 32 scintillator tiles placed at distances $z = 3.3$ m and $z = -0.9$ m from the nominal interaction point, covering the full azimuth within $2.8 < \eta < 5.1$ (VZERO-A) and $-3.7 < \eta < -1.7$ (VZERO-C). Both the amplitude and the time signal in each scintillator are recorded.

^g Now at SUBATECH, Ecole des Mines de Nantes, Université de Nantes, CNRS-IN2P3, Nantes, France;

^h Now at Centro de Investigación y de Estudios Avanzados (CINVESTAV), Mexico City and Mérida, Mexico; Now at Benemérita Universidad Autónoma de Puebla, Puebla, Mexico;

ⁱ Now at Laboratoire de Physique Subatomique et de Cosmologie (LPSC), Université Joseph Fourier, CNRS-IN2P3, Institut Polytechnique de Grenoble, Grenoble, France;

^j Now at Institut Pluridisciplinaire Hubert Curien (IPHC), Université de Strasbourg, CNRS-IN2P3, Strasbourg, France;

^k Now at Sezione INFN, Padova, Italy;

^l Deceased

^m Also at Division of Experimental High Energy Physics, University of Lund, Lund, Sweden;

ⁿ Also at University of Technology and Austrian Academy of Sciences, Vienna, Austria ;

^o Also at European Organization for Nuclear Research (CERN), Geneva, Switzerland;

^p Now at Oak Ridge National Laboratory, Oak Ridge, Tennessee, United States;

^q Now at European Organization for Nuclear Research (CERN), Geneva, Switzerland;

^r Also at Frankfurt Institute for Advanced Studies, Johann Wolfgang Goethe-Universität Frankfurt, Frankfurt, Germany;

^s Now at Frankfurt Institute for Advanced Studies, Johann Wolfgang Goethe-Universität Frankfurt, Frankfurt, Germany;

^t Now at Research Division and ExtreMe Matter Institute EMMI, GSI Helmholtzzentrum für Schwerionenforschung, Darmstadt, Germany;

^u Also at Fachhochschule Köln, Köln, Germany;

^v Also at Institute of Experimental Physics, Slovak Academy of Sciences, Košice, Slovakia;

^w Now at Instituto de Ciencias Nucleares, Universidad Nacional Autónoma de México, Mexico City, Mexico;

^x Also at M.V.Lomonosov Moscow State University, D.V.Skobeltzyn Institute of Nuclear Physics, Moscow, Russia ;

^y Also at Laboratoire de Physique Subatomique et de Cosmologie (LPSC), Université Joseph Fourier, CNRS-IN2P3, Institut Polytechnique de Grenoble, Grenoble, France;

^z Also at "Vinča" Institute of Nuclear Sciences, Belgrade, Serbia ;

^{aa} Also at Wayne State University, Detroit, Michigan, United States;

^{bb} Also at University of Houston, Houston, Texas, United States;

^{cc} Also at Department of Physics, University of Oslo, Oslo, Norway;

^{dd} Also at Variable Energy Cyclotron Centre, Kolkata, India;

^{ee} Now at Department of Physics, University of Oslo, Oslo, Norway;

^{ff} Also at Dipartimento Interateneo di Fisica 'M. Merlin' and Sezione INFN, Bari, Italy;

^{gg} Now at Nikhef, National Institute for Subatomic Physics and Institute for Subatomic Physics of Utrecht University, Utrecht, Netherlands;

^{hh} Also at Institut de Physique Nucléaire d'Orsay (IPNO), Université Paris-Sud, CNRS-IN2P3, Orsay, France;

ⁱⁱ Also at Hua-Zhong Normal University, Wuhan, China;

^{jj} Also at Centro Fermi – Centro Studi e Ricerche e Museo Storico della Fisica "Enrico Fermi", Rome, Italy;

The VZERO time resolution is better than 1 ns, allowing discrimination of beam–beam collisions from background events produced upstream of the experiment. The VZERO also provides a trigger signal. The Zero Degree Calorimeters (ZDCs) measure the energy of spectators (non-interacting nucleons) in two identical detectors, located ± 114 m from the interaction point. Each ZDC consists of two quartz fiber sampling calorimeters: a neutron calorimeter positioned between the two beam pipes downstream of the first machine dipole that separates the two charged particle beams, and a proton calorimeter positioned externally to the outgoing beam pipe. The energy resolution at beam energy is estimated to be 11% for the neutron and 13% for the proton calorimeter, respectively.

For the data analyzed, beams of four bunches, with about 10^7 Pb ions per bunch, collided at $\sqrt{s_{NN}} = 2.76$ TeV, with an estimated luminosity of $5 \times 10^{23} \text{ cm}^{-2}\text{s}^{-1}$. The trigger was configured for high efficiency for hadronic events, requiring at least two out of the following three conditions: i) two pixel chips hit in the outer layer of the SPD, ii) a signal in VZERO-A, iii) a signal in VZERO-C. The threshold in the VZERO detector corresponds approximately to the energy deposition of a minimum ionizing particle. The luminous region had an r.m.s. width of 5.9 cm in the longitudinal direction and $50 \mu\text{m}$ in the transverse direction. The estimated luminosity corresponds to a hadronic collision rate of about 4 Hz. The observed rate was about 50 Hz, mainly due to electromagnetically induced processes [33]. These processes have very large cross sections at LHC energies but generate very low multiplicities and therefore do not contribute to the high particle multiplicities of interest for the present analysis. The trigger rate without beam was negligible and the rate in coincidence with bunches of only one beam was about 1 Hz. This beam background is eliminated from the triggered event sample using the VZERO timing information, as well as the correlation between the number of tracks reconstructed in the Time Projection Chamber (TPC) and the number of hits in the SPD.

Offline event characterization utilizes global event observables that are intrinsically correlated over different regions of phase space through the initial collision geometry. Figure 1 (upper) shows the measured correlation between the energy deposited in the ZDC and the sum of amplitudes in the VZERO detector. The VZERO response is proportional to the event multiplicity, and the ZDC energy to the number of non-interacting nucleons close to beam rapidity. As events become more central, with smaller impact parameter, they generate larger multiplicity in VZERO and less energy forward in the ZDC. This behavior is understood based on collision geometry and nuclear breakup [34]. For small ZDC response the VZERO signal has two distinct values corresponding to peripheral and central collisions. However, the

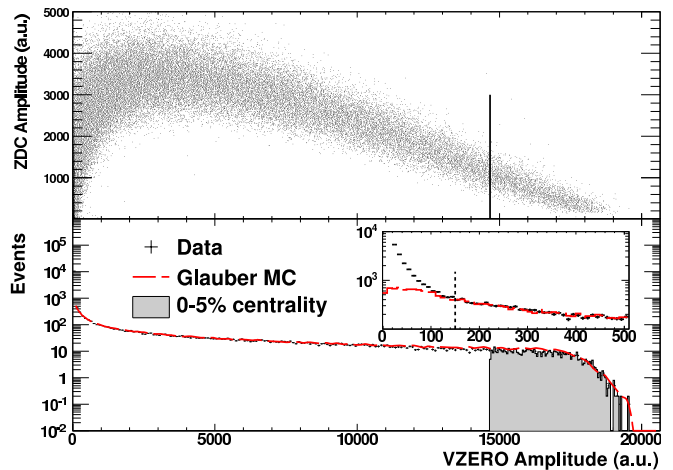


FIG. 1. Upper panel: Correlation of ZDC and the VZERO response in hadronic collisions. Lower panel: Distribution of the sum of amplitudes in the VZERO scintillator tiles (black histogram); inset shows the low amplitude part of the distribution. The red line shows the fit of the Glauber calculation to the measurement. The fit was performed above the cut indicated in the inset, avoiding the region at low amplitudes dominated by the electromagnetic processes. The shaded area corresponds to the most central 5% of hadronic collisions.

VZERO signal alone can be used to discriminate on centrality. Figure 1 (lower) shows the distribution of the VZERO amplitude for all triggered events after beam background removal. The distribution is fit using the Glauber model [35] to describe the collision geometry and a Negative Binomial Distribution (NBD) to describe particle production [34]. In addition to the two parameters of the NBD, there is one free parameter that controls the power-law dependence of particle production on the number of participating nucleons (N_{part}). To avoid the region contaminated by electromagnetic processes, which constitutes over 90% of the triggered events, the fit is restricted to the VZERO amplitude region above 150, where the trigger for hadronic collisions is fully efficient. The fraction of the hadronic cross section from the model fit corresponding to this cut, 87%, allows the determination of the cross section percentile for any more-central VZERO cut by integrating the measured distribution. The most central 5% fraction of the hadronic cross section was determined in this way.

The analysis is based on the VZERO event selection as described above. Among the triggered sample of about 650000 events, 3615 events correspond to the most central 5% of the hadronic cross section, indicated by the shaded region in Fig. 1 (lower). The first step in the measurement of the charged particle multiplicity is the determination of the primary vertex position by correlating hits in the two SPD layers. All events in the central sample are found to have a well-constrained primary ver-

tex. To minimize edge effects at the limit of the SPD

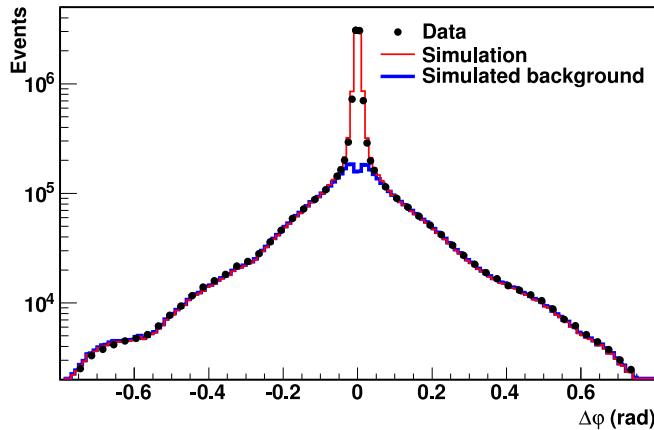


FIG. 2. Distribution of the azimuthal separation ($\Delta\varphi$) of all candidate tracklets in data, simulation, and the background contribution that is estimated from the simulation.

acceptance we have only used events with reconstructed vertex at $|z_{\text{vtx}}| < 7$ cm, reducing the sample to 2711 events. Tracklet candidates [25] are formed using information on the position of the primary vertex and of hits on the SPD layers. A tracklet is defined by a pair of hits, one on each SPD layer. Using the reconstructed vertex as the origin, we calculate the differences in azimuthal ($\Delta\varphi$, bending plane) and polar ($\Delta\theta$, non-bending direction) angles for pairs of hits [31]. Only hit combinations satisfying a selection on the sum of the squares of $\Delta\varphi$ and $\Delta\theta$, each normalized to its estimated resolution (60 mrad in $\Delta\varphi$ and $25\sin^2\theta$ mrad in $\Delta\theta$), are selected as tracklets. If multiple tracklet candidates share a hit, only the combination with the smallest sum of squares of $\Delta\varphi$ and $\Delta\theta$ is kept. The cut imposed on $\Delta\varphi$ efficiently selects charged particles with transverse momentum (p_t) above 50 MeV/ c . Particles below 50 MeV/ c are mostly absorbed by material.

The charged-particle pseudo-rapidity density $dN_{\text{ch}}/d\eta$ is obtained from the number of tracklets within $|\eta| < 0.5$ according to $dN_{\text{ch}}/d\eta = \alpha \times (1 - \beta)dN_{\text{tracklets}}/d\eta$, where α is the correction factor for the acceptance and efficiency for a primary track to generate a tracklet and β is the probability to form a background tracklet from uncorrelated hits. The corrections α and β are determined as a function of the z -position of the primary vertex and the pseudo-rapidity of the tracklet. The simulations used to calculate the corrections are based on the HIJING [36] event generator and a GEANT3 [37] model of the detector response. Three different methods have been used to estimate the combinatorial background.

The main method to estimate the combinatorial background β relies on the event simulation using a sample of events with similar multiplicities (SPD hits) as in the real data. In Fig. 2 the $\Delta\varphi$ distribution for candidate track-

lets is compared for data and simulation. The distributions are very similar, practically identical in the background dominated tails. The second method is based on the injection of random background hits in the real event, in order to evaluate the probability of creating fake tracklets by combinatorics. In the third method events are modified by rotating hits in the inner SPD layer by 180° in φ , thereby destroying real correlations, but preserving global event features. In all cases, the absolute amount of combinatorial background is obtained by matching the tracklet and background distributions in the tails. For the main method, which ideally provides both the shape and the normalization, an adjustment of 1% is needed to match the tails. The estimated combinatorial background is about 14%. In order to account for the effect of the correlated background, the same background subtraction procedure is also applied to the simulation (i.e. without relying on the event generator information). The correction for the acceptance and efficiency, α , is obtained by the ratio of the number of generated primary charged particles to the number of reconstructed tracklets after subtraction of the combinatorial background. In this way, α accounts for geometrical acceptance, detector and reconstruction efficiencies, contamination by weak decay products of strange particles, conversions, secondary interactions and undetected particles below 50 MeV/ c transverse momentum. The overall correction factor α varies slightly depending on vertex position and η , and is about 2.

We have considered the following sources of systematic uncertainties: background subtraction estimated as 2% by comparing the results of different methods; particle composition estimated as 1% by changing the relative abundances of protons, pions, kaons by a factor of two; contamination by weak decays estimated as 1% by changing the relative contribution of the yield of strange particles by a factor of two; low- p_t extrapolation estimated as 2% by varying the amount of undetected particles at low p_t by a factor of two; event generator estimated as 2% by using HIJING [36] with and without jet quenching, as well as DPMJET [38] for the corrections; centrality definition estimated as 3% by using an alternative event selection based on the SPD hit multiplicities, and by varying the range of the Glauber model fit. All other sources of systematic errors considered (tracklet cuts, vertex cuts, material budget, detector efficiency, background events) were found to be negligible. The total systematic errors amounts to 4.8%. Independent cross-checks performed using tracks reconstructed in the TPC and ITS yield results consistent within the systematic uncertainty.

In order to compare bulk particle production in different collision systems and at different energies, and to compare with model calculations, the charged particle density is scaled by the number of participating nucleons, determined using the Glauber model fit described

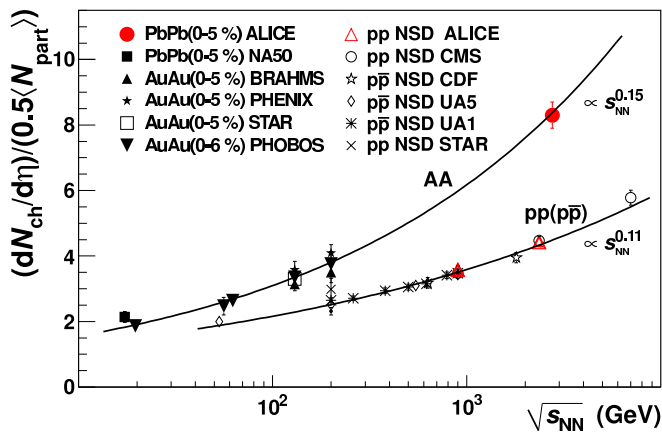


FIG. 3. Charged particle pseudo-rapidity density per participant pair for central nucleus–nucleus [17–25] and non-single diffractive pp ($p\bar{p}$) collisions [26–32], as a function of $\sqrt{s_{NN}}$. The solid lines $\propto s_{NN}^{0.15}$ and $\propto s_{NN}^{0.11}$ are superimposed on the heavy-ion and pp ($p\bar{p}$) data, respectively.

above (Fig. 1). The average number of participants for the 5% most central events is found to be $\langle N_{\text{part}} \rangle = 381$ with an r.m.s. of 18 and a systematic uncertainty of 1%. The systematic uncertainty was obtained by varying the parameters of the Glauber calculation within the experimental uncertainty and by $\pm 8\%$ around 64 mb for the nucleon–nucleon cross section, by using different fit ranges, and by comparing results obtained for different centrality variables (SPD hits, or combined use of the ZDC and VZERO signals).

We measure a density of primary charged particles at mid-rapidity $dN_{\text{ch}}/d\eta = 1584 \pm 4$ (*stat.*) ± 76 (*sys.*). Normalizing per participant pair, we obtain $dN_{\text{ch}}/d\eta/(0.5\langle N_{\text{part}} \rangle) = 8.3 \pm 0.4$ (*sys.*) with negligible statistical error. In Fig. 3, this value is compared to the measurements for Au–Au and Pb–Pb, and non-single diffractive (NSD) pp and $p\bar{p}$ collisions over a wide range of collision energies [17–32]. It is interesting to note that the energy dependence is steeper for heavy-ion collisions than for pp and $p\bar{p}$ collisions. For illustration, the curves $\propto s_{NN}^{0.15}$ and $\propto s_{NN}^{0.11}$ are shown superimposed on the data. A significant increase, by a factor 2.2, in the pseudo-rapidity density is observed at $\sqrt{s_{NN}} = 2.76$ TeV for Pb–Pb compared to $\sqrt{s_{NN}} = 0.2$ TeV for Au–Au. The average multiplicity per participant pair for our centrality selection is found to be a factor 1.9 higher than that for pp and $p\bar{p}$ collisions at similar energies.

Figure 4 compares the measured pseudo-rapidity density to model calculations that describe RHIC measurements at $\sqrt{s_{NN}} = 0.2$ TeV, and for which predictions at $\sqrt{s_{NN}} = 2.76$ TeV are available. Empirical extrapolation from lower energy data [4] significantly underpredicts the measurement. Perturbative QCD-inspired Monte Carlo event generators, based on the HIJING model tuned to

7 TeV pp data without jet quenching [5], on the Dual Parton Model [6], or on the Ultrarelativistic Quantum Molecular Dynamics model [7] are consistent with the measurement. Models based on initial-state gluon density saturation have a range of predictions depending on the specific implementation [8–12], and exhibit a varying level of agreement with the measurement. The prediction of a hybrid model based on hydrodynamics and saturation of final-state phase space of scattered partons [13] is close to the measurement. A hydrodynamic model in

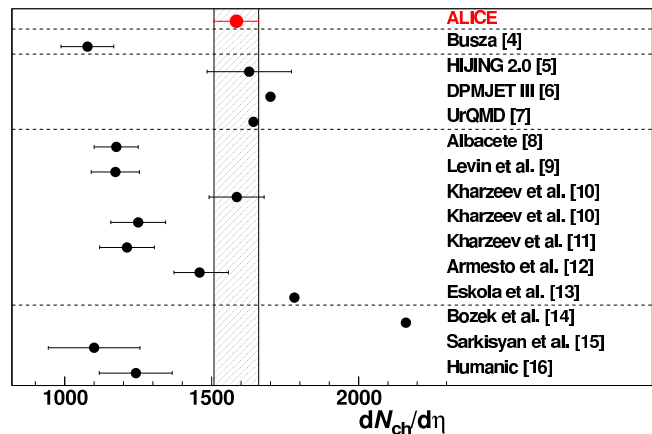


FIG. 4. Comparison of this measurement with model predictions. Dashed lines group similar theoretical approaches.

which multiplicity is scaled from p+p collisions overpredicts the measurement [14], while a model incorporating scaling based on Landau hydrodynamics underpredicts the measurement [15]. Finally, a calculation based on modified PYTHIA and hadronic rescattering [16] underpredicts the measurement.

In summary, we have measured the charged-particle pseudo-rapidity density at mid-rapidity in Pb–Pb collisions at $\sqrt{s_{NN}} = 2.76$ TeV, for the most central 5% fraction of the hadronic cross section. We find $dN_{\text{ch}}/d\eta = 1584 \pm 4$ (*stat.*) ± 76 (*sys.*), corresponding to 8.3 ± 0.4 (*sys.*) per participant pair. These values are significantly larger than those measured at RHIC, and indicate a stronger energy dependence than measured in pp collisions. The result presented in this Letter provides an essential constraint for models describing high energy nucleus–nucleus collisions.

The ALICE collaboration would like to thank all its engineers and technicians for their invaluable contributions to the construction of the experiment and the CERN accelerator teams for the outstanding performance of the LHC complex. The ALICE collaboration acknowledges the following funding agencies for their support in building and running the ALICE detector: Calouste Gulbenkian Foundation from Lisbon and Swiss Fonds Kidagan, Armenia; Conselho Nacional de Desenvolvimento Científico e Tecnológico (CNPq), Financiadora

de Estudos e Projetos (FINEP), Fundação de Amparo à Pesquisa do Estado de São Paulo (FAPESP); National Natural Science Foundation of China (NSFC), the Chinese Ministry of Education (CMOE) and the Ministry of Science and Technology of China (MSTC); Ministry of Education and Youth of the Czech Republic; Danish Natural Science Research Council, the Carlsberg Foundation and the Danish National Research Foundation; The European Research Council under the European Community's Seventh Framework Programme; Helsinki Institute of Physics and the Academy of Finland; French CNRS-IN2P3, the 'Region Pays de Loire', 'Region Alsace', 'Region Auvergne' and CEA, France; German BMBF and the Helmholtz Association; Hungarian OTKA and National Office for Research and Technology (NKTH); Department of Atomic Energy and Department of Science and Technology of the Government of India; Istituto Nazionale di Fisica Nucleare (INFN) of Italy; MEXT Grant-in-Aid for Specially Promoted Research, Japan; Joint Institute for Nuclear Research, Dubna; National Research Foundation of Korea (NRF); CONACYT, DGAPA, México, ALFA-EC and the HELLEN Program (High-Energy physics Latin-American-European Network); Stichting voor Fundamenteel Onderzoek der Materie (FOM) and the Nederlandse Organisatie voor Wetenschappelijk Onderzoek (NWO), Netherlands; Research Council of Norway (NFR); Polish Ministry of Science and Higher Education; National Authority for Scientific Research - NASR (Autoritatea Națională pentru Cercetare Științifică - ANCS); Federal Agency of Science of the Ministry of Education and Science of Russian Federation, International Science and Technology Center, Russian Academy of Sciences, Russian Federal Agency of Atomic Energy, Russian Federal Agency for Science and Innovations and CERN-INTAS; Ministry of Education of Slovakia; CIEMAT, EELA, Ministerio de Educación y Ciencia of Spain, Xunta de Galicia (Consellería de Educación), CEADEN, Cubaenergía, Cuba, and IAEA (International Atomic Energy Agency); The Ministry of Science and Technology and the National Research Foundation (NRF), South Africa; Swedish Research Council (VR) and Knut & Alice Wallenberg Foundation (KAW); Ukraine Ministry of Education and Science; United Kingdom Science and Technology Facilities Council (STFC); The United States Department of Energy, the United States National Science Foundation, the State of Texas, and the State of Ohio.

[1] N. Armesto, (ed.) *et al.*, *J. Phys.* **G35**, 054001 (2008), arXiv:0711.0974 [hep-ph].
 [2] N. Armesto, (2009), arXiv:0903.1330 [hep-ph].
 [3] K. Aamodt *et al.* (ALICE), *J. Instrum.* **3**, S08002 (2008).
 [4] W. Busza, *J. Phys.* **G35**, 044040 (2008), arXiv:0710.2293

[nucl-ex].
 [5] W.-T. Deng, X.-N. Wang, and R. Xu, (2010), arXiv:1008.1841 [hep-ph].
 [6] F. W. Bopp, R. Engel, J. Ranft, and S. Roesler, (2007), arXiv:0706.3875 [hep-ph]; F. Bopp.
 [7] M. Mitrovski, T. Schuster, G. Graf, H. Petersen, and M. Bleicher, *Phys. Rev.* **C79**, 044901 (2009), arXiv:0812.2041 [hep-ph].
 [8] J. L. Albacete, (2010), arXiv:1010.6027 [hep-ph].
 [9] E. Levin and A. H. Rezaeian, *Phys. Rev.* **D82**, 054003 (2010), arXiv:1007.2430 [hep-ph].
 [10] D. Kharzeev, E. Levin, and M. Nardi, *Nucl. Phys.* **A747**, 609 (2005), arXiv:hep-ph/0408050.
 [11] D. Kharzeev, E. Levin, and M. Nardi, (2007), arXiv:0707.0811 [hep-ph].
 [12] N. Armesto, C. A. Salgado, and U. A. Wiedemann, *Phys. Rev. Lett.* **94**, 022002 (2005), arXiv:hep-ph/0407018.
 [13] K. J. Eskola, P. V. Ruuskanen, S. S. Rasanen, and K. Tuominen, *Nucl. Phys.* **A696**, 715 (2001), arXiv:hep-ph/0104010.
 [14] P. Bozek, M. Chojnacki, W. Florkowski, and B. Tomasik, *Phys. Lett.* **B694**, 238 (2010), arXiv:1007.2294 [nucl-th].
 [15] E. K. G. Sarkisyan and A. S. Sakharov, (2010), arXiv:1004.4390 [hep-ph].
 [16] T. J. Humanic, (2010), arXiv:1011.0378 [nucl-th].
 [17] M. C. Abreu *et al.* (NA50), *Phys. Lett.* **B530**, 43 (2002).
 [18] C. Adler *et al.* (STAR), *Phys. Rev. Lett.* **87**, 112303 (2001), arXiv:nucl-ex/0106004.
 [19] I. G. Bearden *et al.* (BRAHMS), *Phys. Lett.* **B523**, 227 (2001), arXiv:nucl-ex/0108016.
 [20] I. G. Bearden *et al.* (BRAHMS), *Phys. Rev. Lett.* **88**, 202301 (2002), arXiv:nucl-ex/0112001.
 [21] K. Adcox *et al.* (PHENIX), *Phys. Rev. Lett.* **86**, 3500 (2001), arXiv:nucl-ex/0012008.
 [22] B. B. Back *et al.* (PHOBOS), *Phys. Rev. Lett.* **85**, 3100 (2000), arXiv:hep-ex/0007036.
 [23] B. B. Back *et al.* (PHOBOS), *Phys. Rev. Lett.* **87**, 102303 (2001), arXiv:nucl-ex/0106006.
 [24] B. B. Back *et al.*, *Phys. Rev. Lett.* **91**, 052303 (2003), arXiv:nucl-ex/0210015.
 [25] B. Alver *et al.*, (2010), arXiv:1011.1940 [nucl-ex].
 [26] C. Albajar *et al.*, *Nucl. Phys.* **B335**, 261 (1990).
 [27] K. Alpgard *et al.*, *Phys. Rev.* **B112**, 183 (1982).
 [28] G. J. Alner *et al.*, *Z. Phys.* **C33**, 1 (1986).
 [29] B. I. Abelev *et al.*, *Phys. Rev.* **C79**, 034909 (2003).
 [30] F. Abe *et al.*, *Phys. Rev.* **D41**, 2330 (1990).
 [31] K. Aamodt *et al.* (ALICE), *Eur. Phys. J. C* **68**, 89 (2010).
 [32] V. Khachatryan *et al.* (CMS), *JHEP* **02**, 041 (2010), arXiv:1002.0621 [hep-ex].
 [33] G. Baur, K. Hencken, D. Trautmann, S. Sadovsky, and Y. Kharlov, *Phys. Rept.* **364**, 359 (2002), arXiv:hep-ph/0112211.
 [34] M. L. Miller, K. Reygers, S. J. Sanders, and P. Steinberg, *Ann. Rev. Nucl. Part. Sci.* **57**, 205 (2007), arXiv:nucl-ex/0701025.
 [35] B. Alver, M. Baker, C. Loizides, and P. Steinberg, (2008), arXiv:0805.4411 [nucl-ex].
 [36] X.-N. Wang and M. Gyulassy, *Phys. Rev. D* **44**, 3501 (1991).
 [37] R. Brun *et al.*, CERN Program Library Long Write-up, W5013, GEANT Detector Description and Simulation Tool (1994).
 [38] S. Roesler, R. Engel, and J. Ranft, (2000), arXiv:hep-ph/0012252.